Taylor & Francis
Taylor & Francis Group

Phase Transitions
A Multinational Journal

ISSN: 0141-1594 (Print) 1029-0338 (Online) Journal homepage: www.tandfonline.com/journals/gpht20

The Jahn–Teller distortion effect on the magnetic properties of the square lattice

Numan Şarlı, Osman Örnek, Hamza Yaşar Ocak & Nihat Arıkan

To cite this article: Numan Şarlı, Osman Örnek, Hamza Yaşar Ocak & Nihat Arıkan (2025) The Jahn–Teller distortion effect on the magnetic properties of the square lattice, Phase Transitions, 98:4-5, 307-313, DOI: 10.1080/01411594.2025.2494217

To link to this article: https://doi.org/10.1080/01411594.2025.2494217

Published online: 24 Apr 2025.

PHASE TRANSITIONS
2025, VOL. 98, NOS. 4–5, 307–313
https://doi.org/10.1080/01411594.2025.2494217

The Jahn–Teller distortion effect on the magnetic properties of the square lattice

Numan Şarlı[a], Osman Örnek[b], Hamza Yaşar Ocak[c] and Nihat Arıkan[d]

[a]Department of Electronic Technology, Osmaniye Korkut Ata University, Osmaniye, Turkey; [b]Department of Materials and Metallurgical Engineering, Ahi Evran University, Kırşehir, Turkey; [c]Department of Physics Teacher Education, Marmara University, İstanbul, Turkey; [d]Department of Medical Services and Techniques, Osmaniye Korkut Ata University, Osmaniye, Turkey

ABSTRACT
In this paper, the Jahn–Teller distortion (JTD) effect on the temperature dependence of magnetization of the square lattice is investigated using the effective field theory developed by Kaneyoshi. We find that the Tc of the square lattice ($\theta = 90°$) is lower than those of z-in ($\theta < 90°$) or z-out ($\theta > 90°$) JTD. Thus, it has a minimum Tc for non-JTD and Tc increases as the JTD increases. Tc-θ curve is conical. However, the square lattice undergoes a magnetic phase transition from ferromagnetic to ferromagnetic at $T < Tc$ and from paramagnetic to ferromagnetic state at the temperature between $Tc^{Sq} < T < Tc^{JTD}$. Therefore, we propose that the JTD has a strong effect on the magnetic properties of the square lattice.

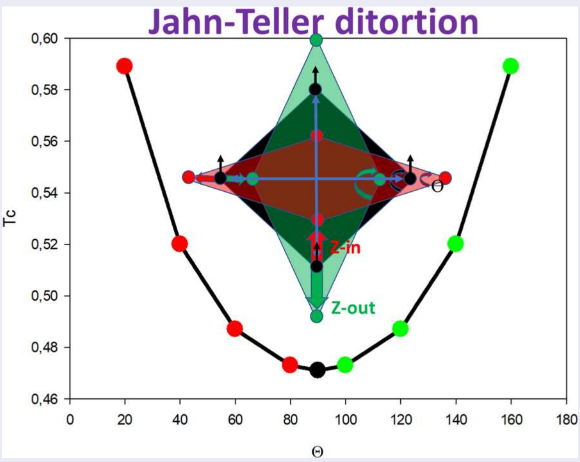

The Jahn–Teller distortion has effects on the Tc of the square lattice.

ARTICLE HISTORY
Received 6 July 2024
Accepted 11 April 2025

KEYWORDS
Jahn-Teller distortion; magnetism; curie temperature: spin; effective field theory

1. Introduction

The Jahn–Teller distortion is predicted in a plane square lattice by Jahn and Teller [1]. They reported that nuclear displacement destroys the fourfold axial symmetry, replacing it with a twofold one. They modeled the distortion with the elongation (z-out) and compression (z-in) in the horizontal plane or vertical plane. These geometrical distortions of molecules and ions are associated

CONTACT Numan Şarlı numansarli1982@gmail.com

with certain electron configurations. When a molecule exhibits a spatially degenerate electronic ground state, it will undergo a geometrical distortion that removes this degeneracy to lower the overall energy of the species [2]. The Jahn–Teller distortion (JTD) or effect (JTE) represents an important phenomenon in physics and chemistry [3]. It was triggered by one of the most important Nobel Prize discoveries in physics of our times inspired by the Jahn–Teller effect: the high-temperature superconductivity. As explained by the authors of this discovery, "the guiding idea in developing this concept was influenced by the Jahn–Teller polaron model". With regard to recent achievements in application to molecular systems, in addition to vast numbers of solutions to structural, spectroscopic and magnetic problems, the Jahn–Teller effect has been most instrumental in explaining the properties of colossal magnetoresistance, the fullerenes, the origin of reactivity and mechanisms of chemical reactions [4,5]. The Jahn–Teller effect is encountered in organic compounds [6,7], transition metal complexes [8], molecule XY_6 [9] and Cu ions [10].

On the other hand, effective field theory (EFT) developed by Takahito Kaneyoshi [11] is one of the very important theories for modeling magnetic systems and obtaining their magnetic properties. For example, nanowires [12], nanotubes [13], graphenes [14, 15], ABO_3-type Perovskites [16] and Heusler alloys [17–21], were modeled and their magnetic properties were investigated. However, some physical phenomena were modeled using KA such as quantum tuneling of magnetization (QTM) [22], exchange bias effect (EBE) [23], Austenite (A), Martensite (M), Detwinned Martensite (DTM) [24] and Bain transformations (BT) [25] and type II superconductivity (SC) [26–30].

Jahn–Teller considered ' … the conditions under which a polyatomic molecule can have a stable equilibrium configuration when its electronic state has orbital degeneracy, i.e. degeneracy not arising from the spin … ' in their famous study [1]. Therefore, in this work, we modeled the JTD with the spin-1/2 Ising particles on the plane square lattice (PSL) and its effects on the temperature

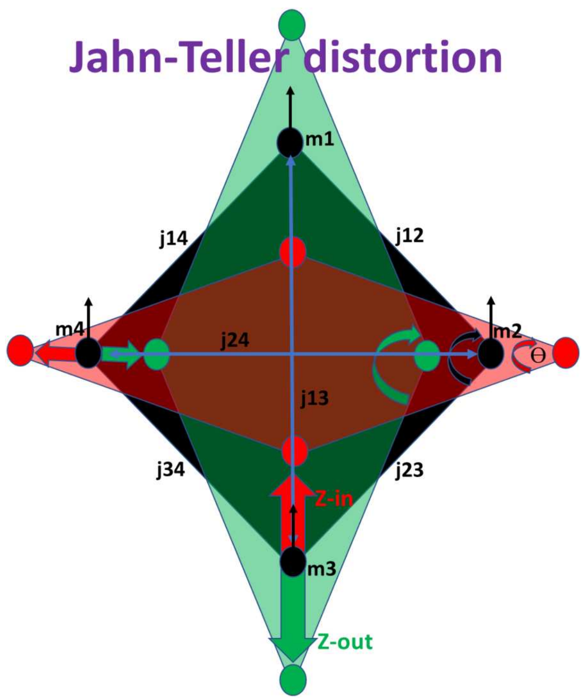

Figure 1. Jahn-Teller distortion in the square lattice (After Ref. [1]).

dependence of magnetization of the PSL (see Figure 1) using the effective field theory (EFT) developed by Takahito Kaneyoshi [11].

2. Model and EFT formulations

We use the effective field theory developed by Kaneyoshi [9] within the Ising model. For the modeling of the JTD (or JTE), we considered the planar square lattice reported by Jahn–Teller [1]. In Figure 1, $m1$, $m2$, $m3$ and $m4$ denote the magnetization of the spin-1/2 Ising particles on the square and distorted square lattice by JTD. $J12$ is the exchange interaction between $m1$ and $m2$ and so on. θ is the twinning angle between two sides of the lattice which defines the direction of the JTD. If the θ is 90°, the lattice is square, if the θ is larger than 90°, the lattice has a z-out JTD and if the θ is lower than 90°, the lattice has a z-in JTD. The Hamiltonian and magnetizations of PSL are given as follows [11]:

2.1. Hamiltonian

$$\begin{aligned} H_{TL} = & -J_{12}\sum_{\langle m1,m2\rangle} S^z_{m1}S^z_{m2} - J_{23}\sum_{\langle m2,m3\rangle} S^z_{m2}S^z_{m3} - J_{34}\sum_{\langle m3,m4\rangle} S^z_{m3}S^z_{m4} \\ & - J_{14}\sum_{\langle m1,m4\rangle} S^z_{m1}S^z_{m4} - J_{13}\sum_{\langle m1,m3\rangle} S^z_{m1}S^z_{m3} - J_{24}\sum_{\langle m2,m4\rangle} S^z_{m2}S^z_{m4} \\ & - H\left(\sum_{m1} S^z_{m1} + \sum_{m2} S^z_{m2} + \sum_{m3} S^z_{m3} + \sum_{m4} S^z_{m4}\right). \end{aligned} \tag{1}$$

In the Hamiltonian, $S^z = \pm 1/2$ shows the Pauli spin operator, and H is the external magnetic field.

2.2. Magnetizations

$$\begin{aligned} m1 = & \left[\cosh\left(\frac{J_{12}\nabla}{2}\right) + 2m_2\sinh\left(\frac{J_{12}\nabla}{2}\right)\right]^1 \left[\cosh\left(\frac{J_{13}\nabla}{2}\right) + 2m_3\sinh\left(\frac{J_{13}\nabla}{2}\right)\right]^1 \\ & \left[\cosh\left(\frac{J_{14}\nabla}{2}\right) + 2m_4\sinh\left(\frac{J_{14}\nabla}{2}\right)\right]^1 F(x)|_{x=0}, \\ m2 = & \left[\cosh\left(\frac{J_{12}\nabla}{2}\right) + 2m_1\sinh\left(\frac{J_{12}\nabla}{2}\right)\right]^1 \left[\cosh\left(\frac{J_{23}\nabla}{2}\right) + 2m_3\sinh\left(\frac{J_{23}\nabla}{2}\right)\right]^1 \\ & \left[\cosh\left(\frac{J_{24}\nabla}{2}\right) + 2m_4\sinh\left(\frac{J_{24}\nabla}{2}\right)\right]^1 F(x)|_{x=0}, \\ m3 = & \left[\cosh\left(\frac{J_{13}\nabla}{2}\right) + 2m_1\sinh\left(\frac{J_{13}\nabla}{2}\right)\right]^1 \left[\cosh\left(\frac{J_{23}\nabla}{2}\right) + 2m_2\sinh\left(\frac{J_{23}\nabla}{2}\right)\right]^1 \\ & \left[\cosh\left(\frac{J_{34}\nabla}{2}\right) + 2m_4\sinh\left(\frac{J_{34}\nabla}{2}\right)\right]^1 F(x)|_{x=0}, \\ m4 = & \left[\cosh\left(\frac{J_{14}\nabla}{2}\right) + 2m_1\sinh\left(\frac{J_{14}\nabla}{2}\right)\right]^1 \left[\cosh\left(\frac{J_{24}\nabla}{2}\right) + 2m_2\sinh\left(\frac{J_{24}\nabla}{2}\right)\right]^1 \\ & \left[\cosh\left(\frac{J_{34}\nabla}{2}\right) + 2m_3\sinh\left(\frac{J_{34}\nabla}{2}\right)\right]^1 F(x)|_{x=0}, \end{aligned} \tag{2}$$

In Equation (2), $\nabla = \partial/\partial x$ used is the differential operator and $F(x)$ is given for the spin-1/2 particles described as follows [11], where k_B is the Boltzmann's constant, $\beta = 1/k_B T_A$.

$$F(x) = \frac{1}{2}\tan h\left[\frac{\beta}{2}(x+h)\right], \tag{3}$$

Finally, the total magnetization of PSL is given as follows

$$MT_{PSL} = \frac{1}{4}(m_1 + m_2 + m_3 + m_4). \tag{4}$$

3. Numerical results

Figure 1 shows the Jahn–Teller distortion effects on the temperature dependence of magnetization of the planar square lattice (PSL). The Curie temperature is obtained at Tc = 0,471 for the square lattice with non-JTD or $\theta = 90°$(black solid line). In Figure 2(a) when JTD starts in the direction of z-out (θ>90°) or z-in ($\theta < 90°$), the Tc of the distorted square lattice is obtained at Tc = 0,589 for elongation ($\theta = 160°$ and green dashed line) and compression ($\theta = 20°$and red solid line). One notes that the non-JTD square lattice has a phase transition from ferromagnetic (FM) to the paramagnetic (PM) phase at $Tc^{Sq} = 0{,}471 < T < Tc^{JTD} = 0{,}589$. Similarly, a phase transition is observed from (FM) to FM phase at $T < Tc^{Sq}$ (see black arrow). Similar behaviors are observed at $Tc^{Sq} = 0{,}471 < T < Tc^{JTD} = 0{,}52$ in Figure 2(b), $Tc^{Sq} = 0{,}471 < T < Tc^{JTD} = 0{,}487$ in Figure 2(c) and $Tc^{Sq} = 0{,}471 < T < Tc^{JTD} = 0{,}473$ in Figure 2(d). The effect of the JTD on the M-T curves of the square lattice disappears when the JTD ends ($\theta = 90°$). These JTD-induced phase transitions agreed with the

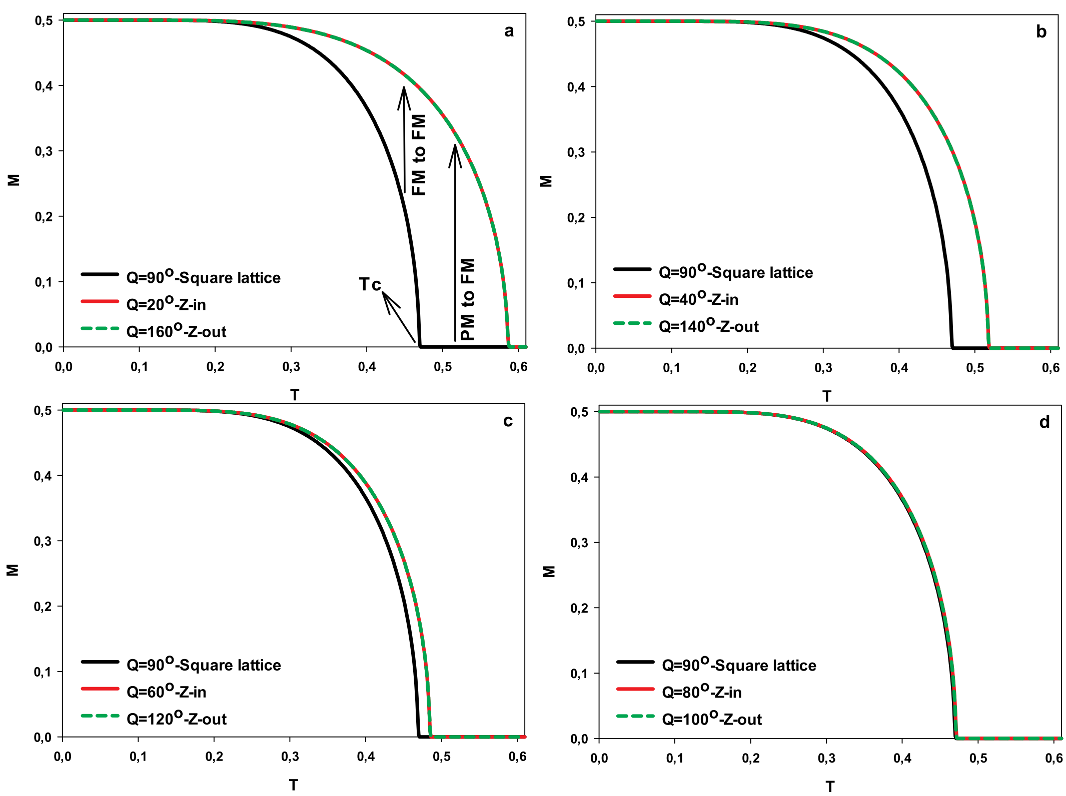

Figure 2. Jahn-Teller distortions effects on the temperature dependence of magnetizations of square lattice at $H = 0$ T; (a) for $\theta = 20°$ and 160°, (b) for $\theta = 40°$ and 140°, (c) for $\theta = 60°$ and 120°, (d) for $\theta = 80°$ and 100°. Tc is the Curie temperature.

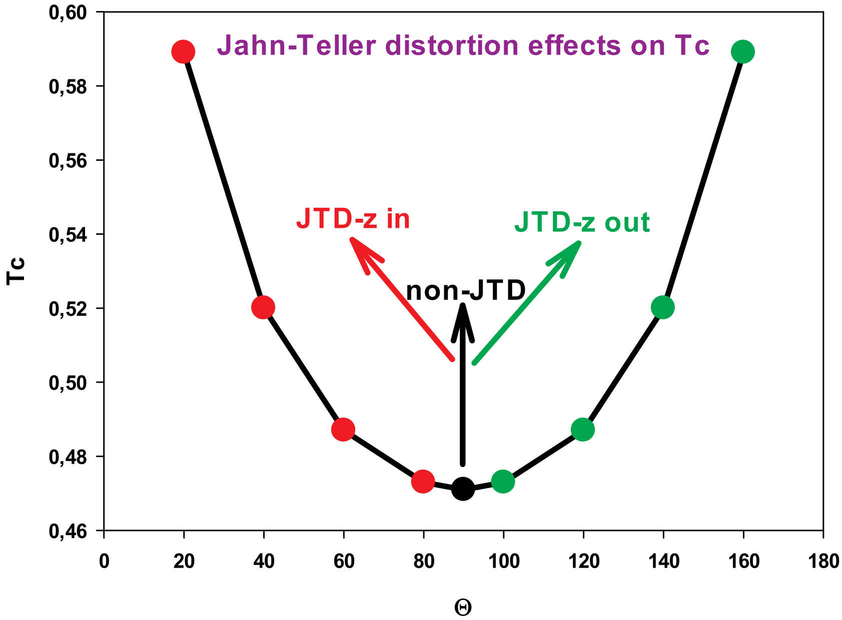

Figure 3. Jahn-Teller distortion effects on Tc of the square lattice.

JTD-induced phase transition from PM to FM of $Pr_{0.6-x}Er_xSr_{0.4}MnO_3$ ($x = 0.0$, 0.1 and 0.2) by M'nassri et al. [31]. They find that all their synthesized samples exhibit a paramagnetic–ferromagnetic transition with decreasing temperature. The magnetic transition temperature T_C decreases continuously with increasing Er concentration. Similarly, magnetic transitions from PM to FM in $LaMn_{1-x}Cr_xO_3$ compounds were observed by Georgalas et al. [32]. Additionally, our M-T results are in good agreement with the M vs T curves for Sr = 0.15, 0.08, 0.07 and 0.06 samples of $La_{0.7}Ca_{0.3-x}Sr_xMnO_3$ ($x = 0.15$, 0.08, 0.07 and 0.06) manganites by Gandara et al. [33]. They find that the Curie temperatures for Sr = 0.15, 0.08, 0.07 and 0.06 samples are 332, 300, 295 and 290 K, respectively. Since the Tc increases as the Sr content increases, we suggest that an increase of Sr content causes JTD in the $La_{0.7}Ca_{0.3-x}Sr_xMnO_3$ and it causes phase transition from PM to FM at 290K < T < 295 K for 0.07, 295K < T < 300 K for 0.08 and 300 K < T < 332 K for 0.15 and from FM to FM at T < Tc = 290 K for 0.07, T < Tc = 295 K for 0.08 and T < Tc = 300 K for 0.15, as shown in Figure 2(a).

Figure 3 shows the Jahn–Teller distortion effects on the Curie temperature (Tc) of the planar square lattice (PSL) for the distortion angles of $\theta = 20°–160°$ with 20° steps. The Tc of PSL has a minimum value for $\theta = 90°$ (non-JTD). On the other hand, when the JTD starts in the direction of z-out ($\theta > 90°$, elongation) or z-in ($\theta < 90°$, compression), the Tc of the distorted PSL increases. Our results of Tc-θ curves are in good agreement with the results of E-d curves and E_I-E_{II} curves of the Jahn and Teller [1]. As they stated

> … it is clear that since the configurations I and II are geometrically congruent and the planes σ', σ in II correspond respectively to the planes σ, σ' in I, the energy of ϕ_σ for the configuration I must be the same as the energy of $\phi_{\sigma'}$ for the configuration II … (see Ref. [1])

Jahn and Teller investigated the orbital degeneracy. In this paper, we investigated the degeneracy arising from the spin-1/2. As a result, we show that the spin degeneracy also gives the same results as orbital degeneracy by Jahn and Teller [1]. On the other hand, the minimum Tc behavior (conic shape) results from JTD in agreement with the effects of Cr-doping on the Jahn–Teller, the orthorhombic to rhombohedral and the magnetic transitions in $LaMn_{1-x}Cr_xO_3$ compounds by Georgalas et al. [32]. They find that As Cr-doping increases, T_{CA} (Magnetic ordering transition temperatures) shows a monotonous decrease from $T_N = 137$ K (for $x = 0.00$) to a minimum at $T_{CA} = 85$ K (for $x = 0.20$). For $x > 0.20$, T_{CA} steadily increases to $T_{CA} = 103$ K for $x = 0.35$, with a diminishing incremental increase. Thus, we suggest the Cr-doping causes JTD in the orthorhombic to rhombohedral $LaMn_{1-x}Cr_xO_3$ compounds as JTD-z out for $x > 0.20$, JTD-z in for $x < 0.20$ and non-JTD for $x = 0.20$, as shown in Figure 1 and Jahn and Teller [1].

4. Conclusions

The Jahn–Teller distortion (JTD) effect on the temperature dependence of magnetization of the square lattice is investigated using EFT (or Kaneyoshi theory [11]), and we find the following.

(1) Planar square lattice has a minimum Tc for non-JTD ($\theta = 90°$)
(2) For the elongation in the direction of z-out ($\theta > 90°$) or compression in the direction of z-in ($\theta < 90°$), the Tc increases.
(3) Our results are in good agreement with the results of orbital degeneracy by Jahn and Teller [1]. Thus, spin degeneracy also gives the same results as orbital degeneracy.
(4) The non-JTD planar square lattice has a phase transition from FM to FM at $T < Tc^{Sq}$ and from PM to FM at $Tc^{Sq} < T < Tc^{JTD}$
(5) There is a strong relationship between the JTD and magnetic properties.
(6) Finally, Jahn and Teller predicted that… Spin degeneracy may also produce similar effects, but these, too, will be small, since the coupling of spin and nuclear motion will depend upon the interaction of the spin with the orbital motion of the electrons, which interaction, at least for light elements, is small …

Our results at the vicinity of $\theta = 90°$ (while the θ goes to 90°), the JTD effect on the M-T and Tc-θ curves is very small, and it disappears at $\theta = 90°$.

Disclosure statement

No potential conflict of interest was reported by the author(s).

References

[1] Jahn HA, Teller E. Stability of polyatomic molecules in degenerate electronic states. I. orbital degeneracy. Proc R Soc A. 1937;161:220–235.
[2] Freitag R, Conradie J. Understanding the Jahn–Teller effect in octahedral transition-metal complexes: a molecular orbital view of the Mn(β-diketonato)$_3$ complex. J Chem Educ 2013;90:1692–1696. doi:10.1021/ed400370p
[3] Breza M. Jahn-Teller phase transitions. Acta Cryst. 1990;46:573–575. doi:10.1107/S0108768190001975
[4] Bersuker I. The Jahn-Teller effect. Cambridge: Cambridge University Press; 2006.
[5] Bednorz JG, Müller KA. In: G Ekspong, editor. Nobel lectures: physics. Singapore: World Scientific; 1993. p. 424.
[6] Senn PA. A simple quantum mechanical model that illustrates the Jahn-Teller effect. J Chem Educ. 1992;69:819–821. doi:10.1021/ed069p819
[7] Johansson AJ. Teaching the Jahn–Teller theorem: a simple exercise that illustrates how the magnitude of distortion depends on the number of electrons and their occupation of the degenerate energy level. J Chem Educ. 2013;90:63–69. doi:10.1021/ed300295r
[8] Klarner F-G. About the anti-aromaticity of planar cyclo-¨ octatetraene. Angew Chem Int Ed 2001;40:3977–3981.doi:10.1002/1521-3773(20011105)40:21<3977::AID-ANIE3977>3.0.CO;2-N
[9] Ham NS. The Jahn-Teller theorem. Spectrochim Acta. 1962;18:775–789. doi:10.1016/0371-1951(62)80082-4
[10] Keller H, Holder AB, Müller AK. Jahn–Teller physics and high-Tc superconductivity. Materialstoday. 2008;11:38–46.
[11] Kaneyoshi T. Differential operator technique in the Ising spin systems. Acta Phys Pol A. 1993;83:703–738. doi:10.12693/APhysPolA.83.703
[12] Şarlı N, Keskin M. Two distinct magnetic susceptibility peaks and magnetic reversal events in a cylindrical core/shell spin-1 Ising nanowire. Solid State Commun. 2012;152:354–359. doi:10.1016/j.ssc.2011.12.015

[13] Şarlı N. Band structure of the susceptibility, internal energy and specific heat in a mixed core/shell Ising nanotube. Physica B. 2013;411:12–25. doi:10.1016/j.physb.2012.08.046

[14] Şarlı N. Generation of an external magnetic field with the spin orientation effect in a single layer Ising nanographene. Physica E. 2016;83:22–29. doi:10.1016/j.physe.2016.04.009

[15] Yıldız YG. Origin of the hardness in the monolayer nanographene. Phys Lett A. 2019;383:2333–2338. doi:10.1016/j.physleta.2019.04.039

[16] Güldal S, Polat Y. Edge and surface antiferromagnetism in ABO_3 perovskite-type nanoparticle within the effective field theory. Philos Mag 2020;100:642–657. doi:10.1080/14786435.2019.1698781

[17] Saatçi B, Şarlı N, Özdemir EG, et al. Bridge constant and atom between theoretical and experimental magnetism in Ni_2MnSb Heusler alloy: DFT and EFT studies. Philos Mag. 2021;101:501–516. doi:10.1080/14786435.2020.1844330

[18] Özdemir EG, Doğruer S, Merdan Z. Electronic, magnetic, half-metallic, pressure-induced elastic and curie temperature predictions of Zr_2RhTl Heusler alloy: DFT and EFT studies. Philos Mag 2024;104:115–135. doi:10.1080/14786435.2023.2285031

[19] Ocak HY, Yıldız GD, Yıldız YG, et al. Transverse field effects of Al concentration on magnetic properties of B2-FeAl nanoparticle. Acta Phys Pol A. 2021;139:20–24. doi:10.12693/APhysPolA.139.20

[20] Yağcı NK. Perpendicular magnetic anisotropy revealed by c/a ratio of Mn2NiB Heusler alloy. J Supercond Novel Magn. 2021;34:959–962. doi:10.1007/s10948-020-05785-8

[21] Malkoç T. A transverse Ising model for the $Fe_{50\text{-}x}Cr_{25}+_xV_{25}$ Heusler alloy. Chin J Phys. 2022;80:378–384. doi:10.1016/j.cjph.2022.11.007

[22] Yıldız GD, Yıldız YG, Şarlı N. Spin induced quantum tunneling of the magnetization. Spin. 2021;11:2150011. doi:10.1142/S2010324721500119

[23] Yıldız YG. Exchange bias effect revealed by irreversible structural transformation between the HCP and FCC structures of Cobalt nanoparticles. Phase Transitions. 2020;93:429–437. doi:10.1080/01411594.2020.1743837

[24] Şarlı N, Paran N, Ablay G, et al. Key role of high-Tc twinned martensitic materials to gain a magnetic actuation higher than 15%. Sens Actuators, A Phys. 2021;332:113136. doi:10.1016/j.sna.2021.113136

[25] Saatçi B, Şarlı N, Dağdemir Y, et al. Prediction of the Bain spin memory materials (BSMM) revealed by Kaneyoshi theory. Philos Mag Lett. 2020;100:330–339. doi:10.1080/09500839.2020.1765264

[26] Keskin M, Şarlı N. Superconducting phase diagram of the yttrium, barium, and YBa-core in YBa2Cu3O7−δ by an Ising Model. J Exp Theor Phys. 2018;127:516–524. doi:10.1134/S1063776118090157

[27] Şarlı N, Keskin M. Effect of the distance range between the YBa-core and CuO-shell on the superconducting properties in the YBCO by an Ising model. Chin J Phys. 2020;63:375–381. doi:10.1016/j.cjph.2019.11.022

[28] Şarlı N, Keskin M. Effects of the copper and oxygen atoms of the CuO-plane on magnetic properties of the YBCO by using the effective-field theory. Chin J Phys. 2020;59:256–264. doi:10.1016/j.cjph.2019.03.007

[29] Keskin M, Şarlı N. Coexistence of ferromagnetism and superconductivity in NiBi-binary alloy. Chin J Phys. 2019;60:502–509. doi:10.1016/j.cjph.2019.05.029

[30] Duran A. Surface superconductivity in Ni50Mn36Sn14 Heusler alloy. J Supercond Novel Magn. 2018;31:4053–4062. doi:10.1007/s10948-018-4686-8

[31] M'nassri R, Cheikhrouhou-Koubaa W, Boudjada N, et al. Structural, magnetic and magnetocaloric properties of $Pr0.6\text{-}xEr_xSr_{0.4}MnO_3$ ($x = 0.0$, 0.1 and 0.2). EPJ Web Conf. 2012;29:00051. doi:10.1051/epjconf/20122900051

[32] Georgalas C, Samartzis A, Biniskos N, et al. Effects of Cr-doping on the Jahn-Teller, the orthorhombic to rhombohedral, and the magnetic transitions in LaMn1-xCrxO3 compounds. Physica B. 2020;586:412101. doi:10.1016/j.physb.2020.412101

[33] Burrola-Gándara LA, Sáenz-Hernández RJ, Santillán-Rodríguez CR, et al. Spin-lattice coupling, Jahn-Teller effect and the influence of the measurement rate in La0.7Ca0.3-xSrxMnO3 manganites. AIP Adv. 2016;6:056219. doi:10.1063/1.4944656